

AD-A031 257

NAVAL WEAPONS SUPPORT CENTER CRANE IND
SELF DIFFUSION IN CEL'S AND TISSUES. (U)
OCT 76 J E TANNER

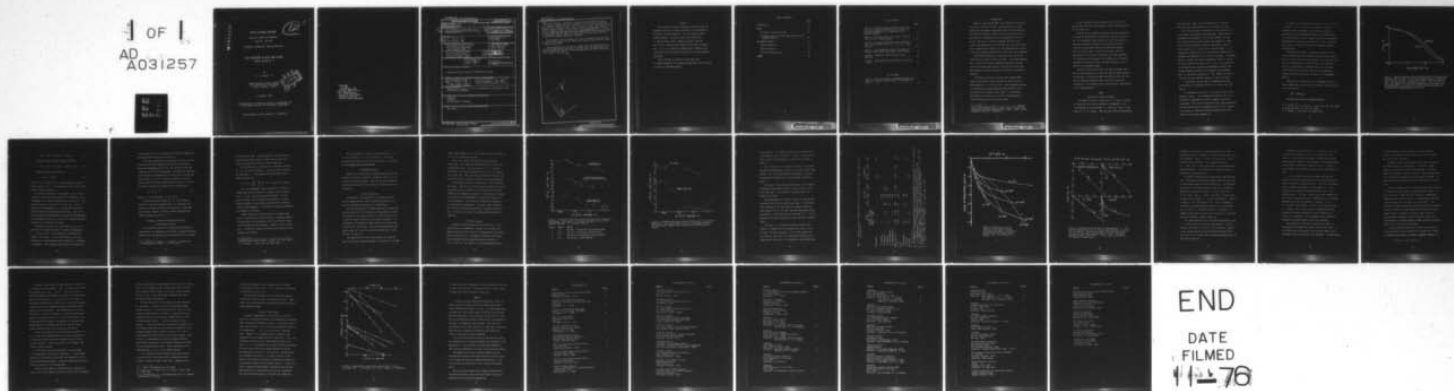
F/G 6/16

UNCLASSIFIED

NWSC/CR/RDTR-42

NL

1 OF 1
AD
A031257



END

DATE
FILMED
11-76

AD A031257

12 FC

OFFICE OF NAVAL RESEARCH

Contract N00014-76-WR60015

Task No. 105-748

TECHNICAL REPORT NO. NWSC/CR/RDTR-42

SELF DIFFUSION IN CELLS AND TISSUES

ANNUAL REPORT NO. 2

by

J. E. Tanner, Jr.

Naval Weapons Support Center
Applied Sciences Department
Crane, Indiana 47522

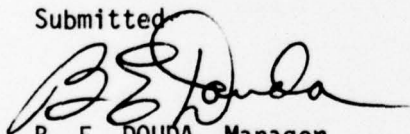


1 October 1976

Reproduction in whole or in part is permitted for
any purpose of the United States Government

Distribution of this report is unlimited

Submitted

A handwritten signature in dark ink, appearing to read 'B. E. Douda', written over the printed name.

B. E. DOUDA, Manager
Chemical Sciences Branch
Pyrotechnic Division
Applied Sciences Department

UNCLASSIFIED

SECURITY CLASSIFICATION OF THIS PAGE (When Data Entered)

REPORT DOCUMENTATION PAGE		READ INSTRUCTIONS BEFORE COMPLETING FORM
1. REPORT NUMBER (14) NWSC/CR/RDTR-42	2. GOVT ACCESSION NO.	3. RECIPIENT'S CATALOG NUMBER
4. TITLE (and Subtitle) (6) SELF DIFFUSION IN CELLS AND TISSUES, Annual Report No. 2	5. TYPE OF REPORT & PERIOD COVERED (9) Annual rept. no. 2 1 July 1975-30 Sep 1976	6. PERFORMING ORG. REPORT NUMBER
7. AUTHOR(s) (10) John E. Tanner, Jr	8. CONTRACT OR GRANT NUMBER(s) N0001476WR60015 of 1 July 1975	
9. PERFORMING ORGANIZATION NAME AND ADDRESS Naval Weapons Support Center ✓ Applied Sciences Department Crane, Indiana 47522	10. PROGRAM ELEMENT, PROJECT, TASK AREA & WORK UNIT NUMBERS 61153N, RR041-20-01, Task No. 105-748	
11. CONTROLLING OFFICE NAME AND ADDRESS Office of Naval Research Medical and Dental Science Arlington, Virginia 22217	12. REPORT DATE (11) 1 October 1976	13. NUMBER OF PAGES 32
14. MONITORING AGENCY NAME & ADDRESS (if different from Controlling Office) (12) 30p.	15. SECURITY CLASS. (of this report) Unclassified	15a. DECLASSIFICATION/DOWNGRADING SCHEDULE
16. DISTRIBUTION STATEMENT (of this Report) APPROVED FOR PUBLIC RELEASE; DISTRIBUTION UNLIMITED		
17. DISTRIBUTION STATEMENT (of the abstract entered in Block 20, if different from Report) (16) RR041-20, NR-105-748 (17) RR041-20-01		
18. SUPPLEMENTARY NOTES Reproduction in whole or in part is permitted for any purpose of the United States Government.		
19. KEY WORDS (Continue on reverse side if necessary and identify by block number) Biophysics Diffusion Nuclear Magnetic Resonance		
20. ABSTRACT (Continue on reverse side if necessary and identify by block number) See reverse		

DD FORM 1 JAN 73 1473

EDITION OF 1 NOV 65 IS OBSOLETE
S/N 0102-014-6601

1

UNCLASSIFIED 409351

SECURITY CLASSIFICATION OF THIS PAGE (When Data Entered)

UNCLASSIFIED

SECURITY CLASSIFICATION OF THIS PAGE(When Data Entered)

The self diffusion coefficient of water has been measured in packed cell samples of human red cells, Escherichia coli, and yeast over a very large range of diffusion times, from 0.3 msec to 1.0 sec. The value at the shortest times is equal or nearly equal to the true cytoplasmic diffusion coefficient, and is 5×10^{-6} cm²/sec for all three samples. This is a factor of three lower than the value previously reported for three different types of frog muscle, and is taken as an indication of greater obstruction by intracellular membranes and other structures.

Measurements of spin relaxation show that reorientation and diffusion of the major portion of the cell water are slowed by about the same amount compared to pure water.

From the diffusion coefficient at longer times, the permeabilities of the outer membranes are estimated to be 0.02 cm/sec for two of the frog muscles and for the red cells, and much higher for the other frog muscle and for the E. coli cells.

ADDITIONAL TO

THIS

DATE FORWARDED

DATE OF REVISION

BY

DISTRIBUTION/AVAILABILITY

DATE

FILE NO. OF

A

UNCLASSIFIED

PREFACE

The frog muscle samples studied here were furnished and prepared by Professor Alfred Strickholm of the Department of Physiology, Indiana University. He also supervised their further handling. The yeast samples were prepared by Dr. Roberto Bastos and Ms. Katherine Assimos using the facilities of Professor Henry Mahler of the Chemistry Department. The *E. coli* sample was prepared by Ms. Margaret Loyd using facilities of Professor Arthur Koch of the Microbiology Department.

Thanks are due to Professor Arthur Clouse and Mr. Robert Addleman, of the Chemistry Department, for assistance in setting up the NMR apparatus.

TABLE OF CONTENTS

	<u>Page</u>
INTRODUCTION	9
THEORY	10
Diffusion in Cellular Systems	10
A Rigorous Formula for Restricted Diffusion with Permeable Barriers	15
EXPERIMENTAL RESULTS	17
Sample Preparation	17
Diffusion Results	18
Relaxation Measurements	30
SUMMARY	32

LIST OF FIGURES

	<u>Page</u>
Figure 1. Relative apparent diffusion coefficient D/D_0 versus reduced diffusion time, $\pi^2 D_0 t/a^2$, for diffusion perpendicular to impermeable, plane parallel barriers	13
Figure 2. Diffusion coefficients versus diffusion time in muscle of <u>Rana pipiens</u>	19
Figure 3. Diffusion coefficient versus diffusion time in well-packed samples of E. coli and of human red cells	20
Figure 4. Echo attenuation versus the product of diffusion and gradient squared for a yeast sample . .	23
Figure 5. Examples of the variation of echo amplitude	24
Figure 6. Representative signal decay curves due to T_1 and T_2	31

LIST OF TABLES

Table 1. Diffusion constants, membrane permeabilities, and spin relaxation times of water in four types of cells	22
--	----

INTRODUCTION

Magnetic field gradient NMR is well adapted to measuring diffusion in colloidal systems, including biological cells, because the experimental measurement times by this method are such that the distances traveled by the molecules are of the same order as the dimensions of the inhomogeneities of the system. The result is that the apparent diffusion coefficients are dependent on the diffusion time. By varying this latter parameter the dimensions of the inhomogeneities as well as the local diffusion coefficients within them can be obtained.

The maximum information is obtained by the use of the widest possible range of diffusion times. In the work reported here, a variety of recently developed techniques have been used to get a much wider range of diffusion times than have been employed in previous studies of diffusion in biological materials.

The theory of the use of pulsed field gradient NMR to measure intracellular self diffusion has been outlined in Annual Report No. 1¹ of this project. The equipment necessary for performing such experiments has been assembled, and a description was included in that report. A preliminary description of the results of a series of measurements on various frog muscles was also given there.

¹ J. E. Tanner, *Self Diffusion in Cells and Tissues*, NWSC/CR/RDTR-6, Naval Weapons Support Center, Crane, IN (June 1975). Available Defense Documentation Center (DDC), Cameron Station, Alexandria, VA 22314. AD-A014601.

In the intervening time, the data on three systems of packed single cells has been worked up, and a complete account will be given here.

Portions of the experimental results have been presented at the March 1976 Meeting of the American Physical Society, at the 17th Experimental NMR Conference in April 1976, and at a symposium on Magnetic Resonance in Colloid and Interface Science at the national meeting of the American Chemical Society in August 1976. A preliminary written draft for publication in a scientific journal has also been completed. It includes not only the work of the author, but all previous experimental diffusion results from the literature, using a magnetic field gradient method.

During the course of the year the need has become clear for a rigorous derivation of the relationship between diffusion coefficients, as measured by NMR, and diffusion time, for the case of diffusion through periodic barriers of arbitrary permeability. Preliminary work at deriving such a relationship will be indicated here.

THEORY

Diffusion in Cellular Systems

The apparent diffusion coefficient, D , of water in systems of biological cells may be expected to be dependent on the time allowed for the measurement, t_D , when this time is in the range 10^{-4} to 10^0 seconds. NMR spin-echo diffusion measurements

fall within this range, and the expectation of a variable diffusion coefficient has been verified a number of times.

One of the structures responsible for the variation in D is the outer cell membrane, the plasmalemma. When diffusion experiments are performed in a time short enough such that most of the molecules do not contact this membrane, D represents the true cytoplasmic diffusion coefficient, which we refer to here as D_0 . As the time of the experiment, t_0 , is lengthened a larger fraction of the molecules contact the cell membranes and experience their restrictive effects. D decreases, and as t_0 becomes very large D approaches a limit, D_∞ , which is readily shown to be given by $1/D_\infty \approx 1/D_0 + 2/aP$, where a is the average distance between outer membranes (actually the average component parallel to the magnetic field gradient), and P is the barrier permeability. This relation is exact in the limit that the membrane thickness is much less than a .

It can readily be seen that for impermeable barriers $D_\infty=0$, whereas for permeable barriers D_∞ is finite, but less than D_0 .

At intermediate values of t_0 it is obvious that D lies between D_0 and D_∞ . Exact mathematical relations for D vs t_0 , for barriers (membranes) of specific geometry, are quite complicated. Most such relationships as have been derived are for the limiting case of impermeable barriers, $P=0$. There is in existence no rigorously derived relationship valid for barriers of arbitrary permeability.

An example of the relationship between D and t is given in Figure 1. This is for the case of diffusion between regularly spaced, impermeable planar barriers, where D is measured by the pulsed gradient method, and the duration of the gradient pulses is small compared to the time required for the molecules to diffuse across the cells. Such is the case here, and this relation will be used to evaluate the data presented here.

Although we do not have a rigorous expression for the diffusion coefficient with permeable barriers, we will make a guess so as to be able to treat the data. We assume that the form of the expression is similar to that for impermeable barriers, and proceed by a superposition of the diffusion coefficient at long diffusion times and a time-dependent diffusion coefficient as given for the case of impermeable barriers.

Nearly all of the derivations for impermeable barriers of various geometries, with pulsed or continuous field gradient,²⁻⁴ can be expressed as

$$D/D_0 = f(D_0 t, a).$$

We might thus write for permeable barriers:

²J. E. Tanner and E. O. Stejskal, J. Chem. Phys. 49, 1768 (1968).

³B. Robertson, Phys. Rev. 151, 273 (1966).

⁴C. H. Neuman, J. Chem. Phys. 60, 4508 (1974).

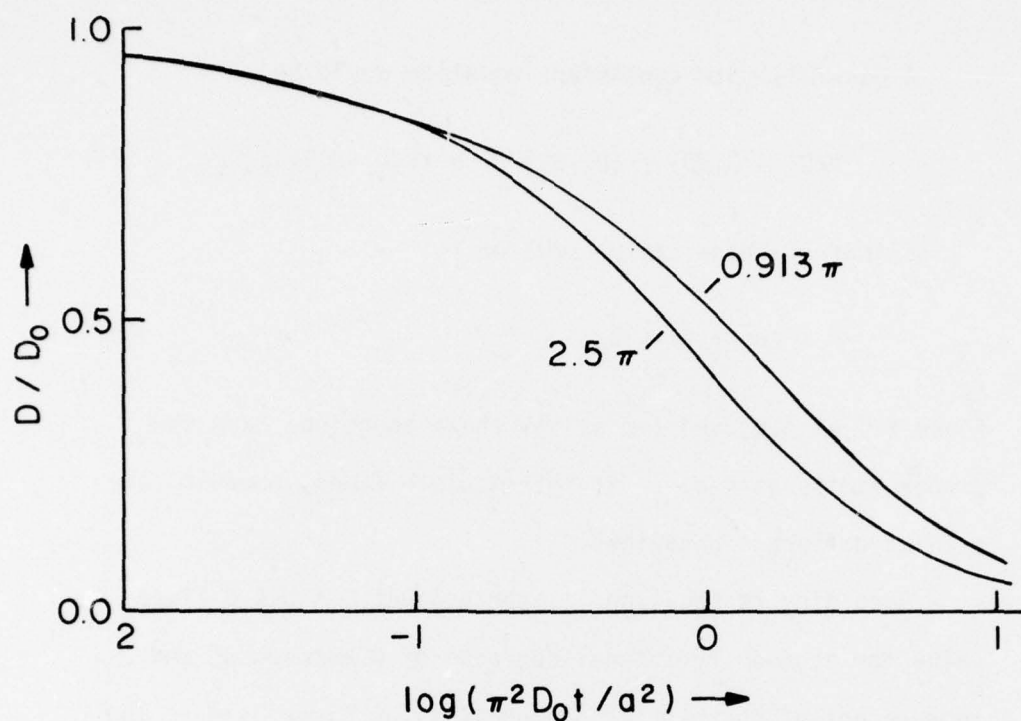


Figure 1. Relative apparent diffusion coefficient D/D_0 versus reduced diffusion time, $\pi^2 D_0 t / a^2$, for diffusion perpendicular to impermeable, plane parallel barriers. The two curves are at different values of $\gamma \delta g a$. The upper curve is appropriate to the *E. coli*, red cell, and yeast measurements. Curves in the neighborhood of the lower curve are appropriate to the values of δ and g used for measurements on frog muscle at intermediate diffusion times.

$$D/D_0 = D_\infty/D_0 + (D_0 - D_\infty)/D_0 \times f(D_0 t, a). \quad (1)$$

A possibly more consistent equation would be

$$D/D_0 = D_\infty/D_0 + (D_0 - D_\infty)/D_0 \times f[(D_0 - D_\infty)t, a]. \quad (2)$$

Either of these can be written as

$$D = fD_0 + (1-f)D_\infty. \quad (3)$$

Since $f \rightarrow 1$ as $t \rightarrow 0$, and $f \rightarrow 0$ as $t \rightarrow \infty$ these equations have the proper limits at $t=0, \infty$. At intermediate times, however, they predict different behaviors.

According to Equation (1) the product $D_0 t$ has a fixed value for a given fractional decrease of D between D_0 and D_∞ , independent of the barrier permeability as given by D_∞ . The average distance of diffusion as if free, $x_{rms} = (2D_0 t)^{1/2}$, would also be independent of D_∞ , as would the fraction of molecules which had encountered the barriers. Thus, $(1-f)$ could be taken as representing the fraction of molecules which had encountered the barriers, and $(D_0 t)^{1/2}$ could be taken as a characteristic length for the system.

According to Equation (2), the product $(D_0 - D_\infty)t$ at a particular fractional decrease of D would be independent of D_∞ . Then $[(D_0 - D_\infty)t]^{1/2}$ could represent a characteristic length of the system. It can be seen that x_{rms} for free diffusion as calculated above would increase as D_∞ increased at constant f . This would be qualitatively consistent with

the assumption that $(1-f)$ represents the fraction of molecules which have been reflected by the barriers.

I find the assumption that the fractional decrease of the diffusion coefficient depends on the fraction of molecules which have encountered the barriers more plausible than that it depends on the fraction reflected. The degree of reflection should determine the magnitude of the effect on D , but not the time at which it sets in. Therefore, Equation (1) will be used to analyze the data presented here; and using f as given by Figure 1, the barrier distance will be calculated as

$$\underline{a} \approx \pi(D_0 t_{1/2})^{1/2}, \quad (4)$$

where $t_{1/2}$ is the time when $D = (D_0 + D_\infty)/2$.

It may be noted that Cooper, et. al.⁵ have proposed Equation (3) with the assumption that $(1-f)$ represents the fraction of molecules deflected by the barriers. With some inconsistency, however, they then calculate characteristic lengths proportional to $(D_0 t_{1/2})^{1/2}$.

A Rigorous Formula for Restricted Diffusion with Permeable Barriers

Our uncertainty about how to analyze diffusion data for permeable barriers emphasizes the need for a rigorously derived expression for the apparent diffusion coefficient as a function

⁵ R. L. Cooper, D. B. Chang, A. C. Young, C. J. Martin, and B. Ancker-Johnson, *Biophys. J.* 14, 161 (1974).

of the diffusion time. Three approaches for deriving such an expression have been explored in detail and at least two of them are believed to be feasible, though cumbersome.

The basic problem is to derive the distribution function $P(x_0|x, t_0)$ after an arbitrary t_0 for spins which started at the same point, x_0 . The apparent diffusion coefficient is then calculated from

$$D = (1/t_0) \ln \int_{-\infty}^{\infty} \int_{-\infty}^{\infty} P(x_0|x, t_0) \cos[\gamma \delta g(x-x_0)] dx dx_0 .$$

One of the approaches under consideration is based on a scheme taken from the diffusion literature for calculating $P(x_0|x, t_0)$ for a physically appropriate model.⁶ At this point it appears that an algebraic expression will not be obtained--numerical calculations must be made for selected values of the parameters. This method is now being programmed for computer calculations.

Another approach is a modification of a concept used earlier to describe restricted diffusion.⁷ Separate algebraic solutions which are approximately valid for different ranges of the variables may be obtainable. However, they are cumbersome. In addition, there are problems with a physical interpretation of the model.

⁶M. Necati Ozisik, *Boundary Value Problems of Heat Conduction* (International Textbook Company, Scranton, PA, 1963), Chpt. 6.

⁷E. O. Stejskal, *J. Chem. Phys.* 43, 3597 (1965).

The third approach is based on constructing $P(x_0|x, t_0)$ as a sum of segments of a Gaussian function. A method of performing the summation has been found; however, the validity of this approach must be established.

EXPERIMENTAL RESULTS

Workup of the diffusion and relaxation data taken in the previous fiscal year on samples of human red cells, *E. coli*, and yeast has been completed. These results are reported and discussed here along with the previously presented results on frog muscle.

Sample Preparation

The procedure for preparation of the samples will be briefly summarized here, with a detailed explanation to be given in the publication presently in preparation.

The frog muscles were dissected from freshly pithed frogs and kept alive until the completion of measurements, at which time they were tested with electrical stimuli and found to be in nearly as good a condition as just after dissection. The confinement of the NMR glass sample tube kept them stretched to nearly their full length. The diffusion measurements were made at about 27°C, and in a direction perpendicular to the long axis of the cell.

The human red cells were freshly drawn from a healthy adult into sterile, heparinized tubes, transferred to 5 mm NMR

tubes, centrifuged to 51% of the original volume, and measured at 27°C over a three hour period.

The *E. coli* culture, strain ML308, was washed and centrifuged. The sludge was blotted and quickly packed into the NMR sample tube. The measurements, at 27°C, required seven hours. The sample generated about 30% of its volume of gas in this time. The cells were observed to be intact at the end of this period, though no viability tests were performed.

Two different cultures of haploid yeast, strain X2180-1B, were grown. The first was centrifuged and blotted; the second culture was suction filtered in several batches for varying lengths of time (degrees of dryness). One portion was treated in a solution of glutaraldehyde to crosslink the protein on the cell membrane. A portion of one sample was cultured at the completion of measurements. The colony count indicated 100% viability, though the uncertainty is perhaps a factor of two. A similar test on the crosslinked sample showed zero viability.

Diffusion Results

The entire diffusion data from the frog muscle, *E. coli*, and red cells are summarized in Figures 2 and 3, where the apparent diffusion coefficients are plotted against the experimental diffusion times. The apparent diffusion coefficients were calculated from the experimental data according to $\ln R = -\gamma^2 D g^2 \delta^2 (\Delta - \delta/3)$, where R is the echo attenuation due

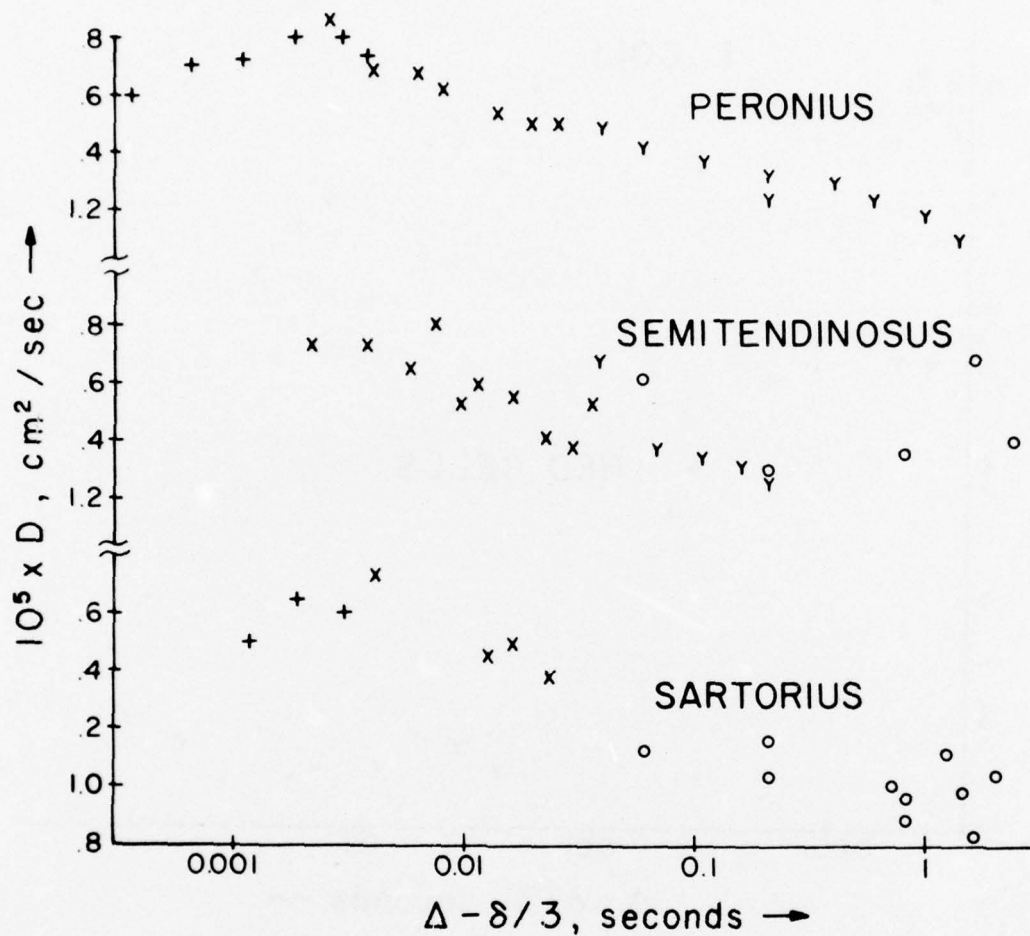


Figure 2. Diffusion coefficients versus diffusion time in muscle of *Rana pipiens*. Each point is an average of values at 2 to 5 field gradient strengths. In all cases $\delta=0.4$ msec.

Symbols	Samples	Method
+	1,2	90°-180°, alternating sign gradient pulses
x	1,2,3	90°-180°, conventional gradient pulses
y	2,3	90°-90°-90°, conventional gradient pulses
o	4,5	90°-90°-90°, steady gradient

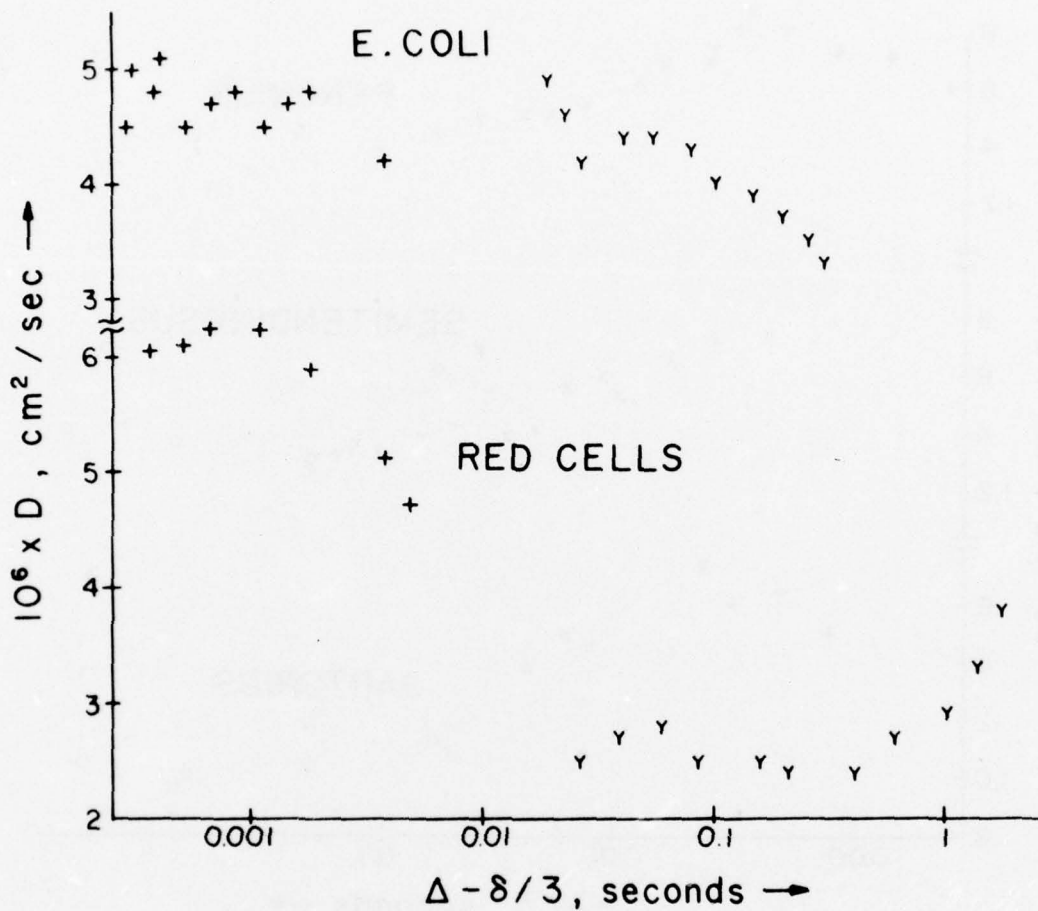


Figure 3. Diffusion coefficient versus diffusion time in well-packed samples of *E. coli* and of human red cells. The symbols indicate the type of pulse sequence used, and have the same meaning as in Figure 2.

to the gradient. The intensity, duration, and separation of the gradient pulses are given by g , δ , and Δ , respectively. A sample of diffusion measurements in yeast are presented in Figure 4.

Each of the points in the plots of Figures 2 and 3 were obtained from measurements at two to five values of the field gradient. For a few representative measurements, the echo attenuations are plotted versus field gradient squared in Figure 5.

The values of the diffusion coefficients at the longest and shortest experimental diffusion times, as well as the T_2 (spin-spin) and T_1 (spin-lattice) relaxation times, are summarized in Table 1.

The measurements for red cells (Figure 3) give the best coverage of the diffusion coefficient range. The diffusion times extend well into the regions of constant diffusion coefficients D_0 and D_∞ , at short and long measurement times, respectively. (The upward trend of the data at $t_D \gg 1$ sec is probably an artifact induced by the very low signal strength there.)

The time, $t_{1/2}$, at which the diffusion coefficient reaches its midpoint may be estimated from Figure 3 to be 6.5 msec. We then calculate $\underline{a} = 6.3 \mu\text{m}$ from Equation (4). This value is large, but still reasonable considering the dimensions of the red cell. We expected a value larger than

TABLE 1. Diffusion constants, membrane permeabilities, and spin relaxation times of water in four types of cells.

	$10^5 \times D$ (cm^2/sec) at the shortest times	This work		Literature		Dry wt.
		T (msec)	T (msec)	$10^5 \times D$ (cm^2/sec)	P (cm/sec)	
Frog muscle						30%
#1 sartorius	1.6		1400			1.1 ^b
#4 sartorius		45 ^a	1000	0.02		1.6 ^c
#2 peronius	1.7	52	1100	0.02		
#3 semitendinosus	1.7	55	1100			
#5 semitendinosus			1400			
Human red cells	0.62	80 ^a	770	0.015 ^e	0.005	28% ^g
E. coli	0.48	25	590	1		26%
Yeast						
centrifuged	0.5	31	460			
filtered	0.6	33 ^a	390			29%
Pure water	2.3	2.3			2.41 ^f	

a. The same result within an uncertainty of $\pm 5\%$ was obtained using a 90° - 90° or a 90° - 180° ref pulse sequence.

b. E. D. Finch, J. F. Harom and B. H. Muller, Arch. Biochem. Biophys. 147, 299 (1971).

c. L. A. Abetsedarskaya, F. G. Miftakhutdinova, and V. D. Fedotov, Biophysics 13, 750 (1968).

d. R. L. Cooper, D. B. Chang, A. C. Young, C. J. Martin, and B. Ancker-Johnson, Biophys. J. 14, 161 (1974).

e. Calculated from M. Shporer and M. Civan, Biochim. Biophys. Acta 335, 31 (1975).

f. R. Mills, J. Phys. Chem. 77, 685 (1973).

g. D. Savitz, V. Sidel, and A. K. Solomon, J. Gen. Physiol. 48, 79 (1964).

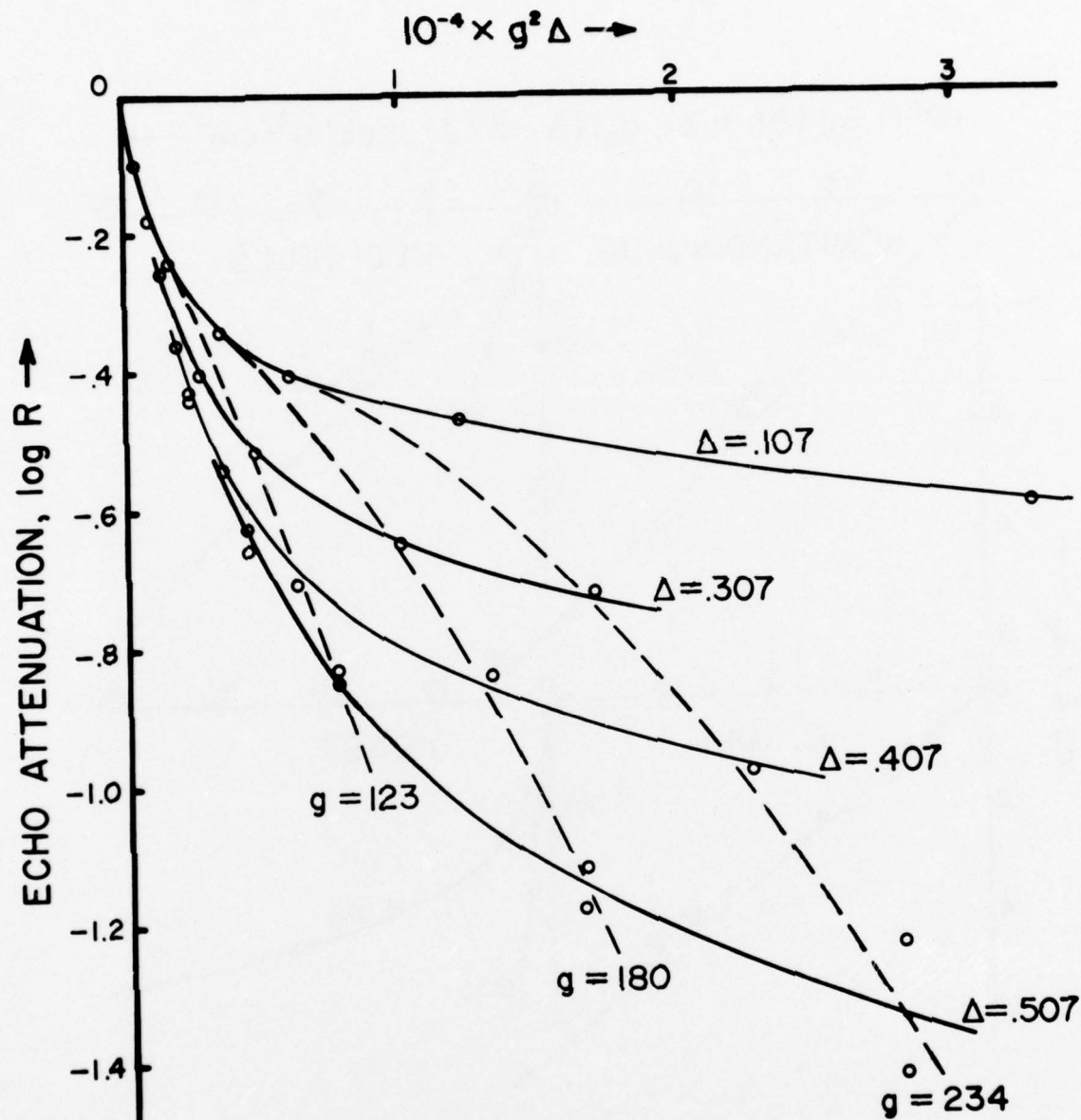


Figure 4. Echo attenuation versus the product of diffusion time and gradient squared for a yeast sample. The solid lines are at constant diffusion time in seconds. The dashed lines are at constant field gradient in G/cm. The pulse width, δ , is constant.

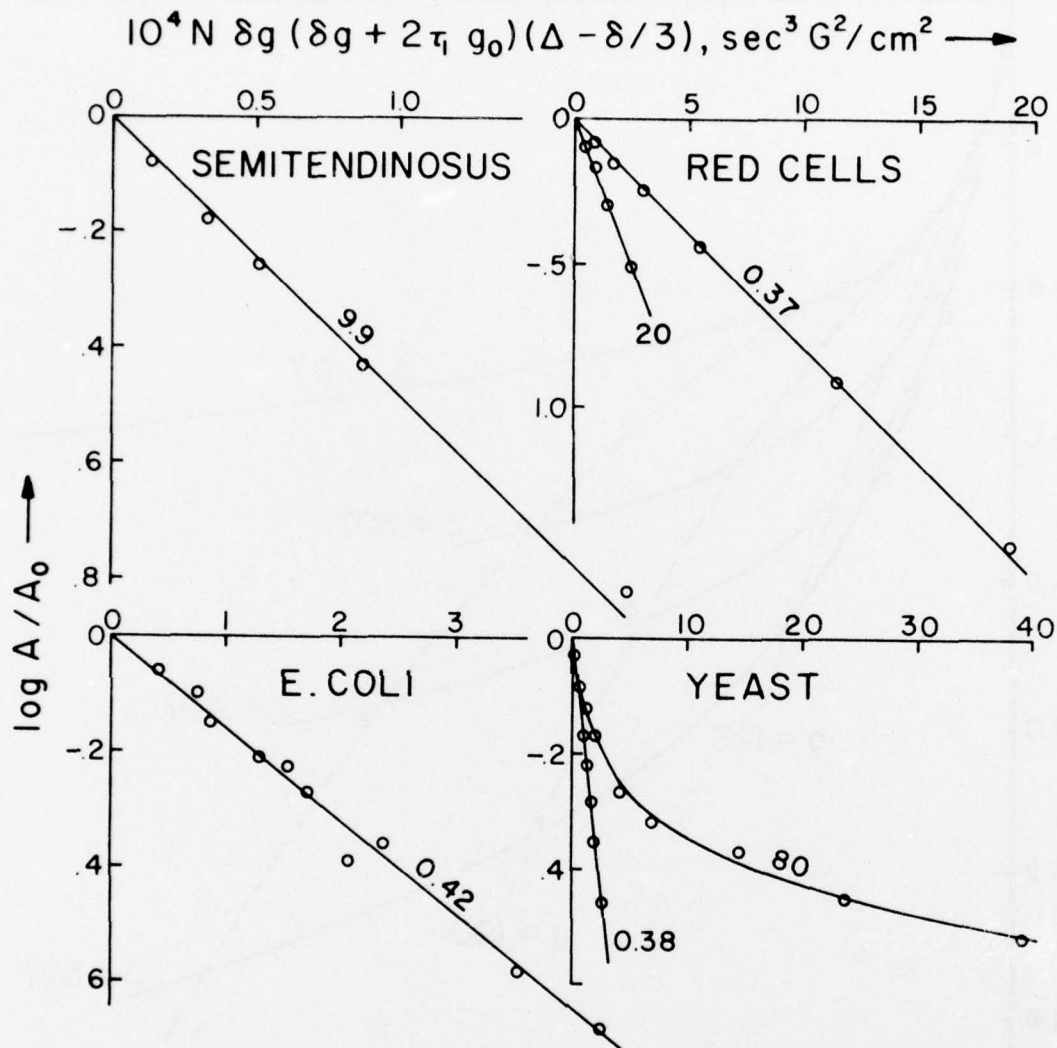


Figure 5. Examples of the variation of echo amplitude, A , versus field gradient squared, g^2 , at constant diffusion time, $\Delta - \delta/3$, for the cell samples. The diffusion times in msec are indicated on the curves. The slopes may be divided by 3.1×10^9 to give the apparent diffusion coefficients. δ , N , g_0 , and τ_1 , as well as Δ are constant for each curve.

a geometric average over all orientations because of the deflection effects of membranes at oblique orientations to the field gradient. With $D_0 = 6.2 \times 10^{-6}$ cm²/sec and $D_\infty = 2.6 \times 10^{-6}$ cm²/sec we then calculate $P \approx 0.015$ cm/sec from $1/D_\infty = 1/D_0 + 2/aP$. This is the minimum that can be calculated from these measurements. The selection of a smaller value of a would yield a larger value of P .

The cells of frog muscles are much larger than red blood cells, and there was difficulty extending the diffusion times to large enough values to directly measure D_∞ . Assuming that the values at the longest times are close to D_∞ we have for peronius and sartorius muscles $D_\infty = 1.2 \times 10^{-5}$ and 1.0×10^{-5} cm²/sec, resp., and $D_0 = 1.7 \times 10^{-5}$ and 1.6×10^{-5} cm²/sec, resp. In both cases we obtain $t_{1/2} \approx 50$ msec from Figure 2. Then we estimate $a = 28$ μ m from Equation (4). This is reasonable, considering the known diameter of about 70 μ m at the widest point in the cell. We then calculate $P = 0.02$ cm/sec. A somewhat larger value of a and smaller value of D_∞ might have been used, yielding a smaller value of P .

With semitendinosus muscle the difference between D_0 and D_∞ is smaller than its precision of measurement, so that a numerical calculation of a and P is not justified. However, we can see qualitatively that the membrane permeability of this muscle is much larger than the membrane permeabilities of the other two muscles.

Probably the major uncertainty in calculating P for all of these muscle samples results from the relatively small change in D over a very large change in diffusion times and hence apparatus settings. For the sartorius and semitendinosus muscles there is additional uncertainty due to a change in sample between the experiments at short and at long diffusion times.

E. coli was the smallest cell studied, and here the problem was to obtain measurements at short enough diffusion times so as to get a good value for D_0 . The cells are approximately cylinders of diameter $1\text{ }\mu\text{m}$ and length $3\text{ }\mu\text{m}$. From Equation (4) we expect the transition from D_0 to D_∞ to be centered near $t_D = 1/2\text{ msec}$. Only a very slight change can be seen in this region of the plot, indicating a very large water permeability of the cell membrane. Taking $a = 1.0\text{ }\mu\text{m}$, $D_0 = 5.0 \times 10^{-6}\text{ cm}^2/\text{sec}$ and $D_\infty = 4.5 \times 10^{-6}\text{ cm}^2/\text{sec}$ we calculate $P = 1\text{ cm/sec}$. This is only an order of magnitude estimate because of the large uncertainty in the difference $D_0 - D_\infty$. Even so it is enormous. This measurement should probably be repeated with another sample, dried more thoroughly.

The sharp drop in diffusion coefficient at longer t_D corresponds to distances much larger than the cell sizes. It is believed due to gas bubbles, which occupied about $1/3$ of the sample volume at the end of the experiment. The measurements

at long diffusion times were taken last. An instrumental artifact is considered unlikely because the signal strength was still fairly strong here.

Altogether, four different yeast samples were observed in an extensive series of measurements. The results, though unusual in several ways, were fairly consistent. A typical example of the data is given in Figure 4. The echo attenuations are plotted versus diffusion time times gradient squared. It was not possible to calculate diffusion coefficients from the data.

The first feature which is striking is the strong curvature of logarithm of echo attenuation versus gradient squared. For observations on a single molecular species in a homogeneous medium such plots must be linear. In inhomogeneous media nonlinearities may arise, but they are usually small.² The existence of several observable species with markedly different diffusion coefficients would explain this particular feature. However, there is probably no molecular species present in concentrations comparable to that of water in yeast cells. The existence of isolated regions of water of greatly differing mobilities is also not very plausible.

A second unusual feature of the results is that at any point the change in echo attenuation is greater for a change in diffusion time than for a change in gradient squared, i.e.,

$$d \ln R / d \ln \Delta > d \ln R / d \ln g^2.$$

The manner of performing the experiments was to keep the relaxation constant by keeping τ_1 and τ_2 constant while varying the gradient, but to vary τ_1 with t_D . Thus, these results could be mathematically modeled by a mixture of two detectable species with different T_1 's, the species with the longer T_1 having the higher diffusion coefficient. In the actual physical situation, regions of absorbed and non-absorbed water would show just such a difference. The absorbed water should have the shorter T_1 and also the lower D . However, absorbed water generally constitutes too small a fraction of the total (<10%) to show the effect observed. Furthermore, the exchange times between regions are probably much shorter than the experimental diffusion times, so as to wipe out this effect.

Possible experimental artifacts have been considered. In one run there was independent reason to suspect superposition of the observed echo and the free induction decay from the previous 90° pulse. After correction for this, however, the unusual features remained.

Thus the yeast data are unexplained. The experiments will be repeated at the earliest opportunity. A lower temperature will be employed to insure that cell degradation is not occurring during measurements. Additional apparatus precautions and cross checks will also be employed.

Turning to the summary of diffusion results presented in Table 1, the column labeled "diffusion at short times" represents

diffusion coefficients at experimental times of 0.3 to 0.5 msec, which is short enough so that the restrictive effect of the outer membrane should be small in all cases, except possibly that of *E. coli*. Thus, these values represent true intracellular diffusion coefficients.

First we see that all of the values are lower than that for pure water. The water content of these samples ranges between 65 and 75%. Since much of the solids consist of high molecular weight proteins, cytoplasm is somewhat similar to ordinary solutions of high molecular weight polymers in low molecular weight solvents. In previous studies of such systems^{8,9} it has been found that the presence of about 30% of the soluble polymer decreases the diffusion constant of a low molecular weight solvent by about a factor of x2. This is approximately the effect found in the cellular systems. Thus we feel it is reasonable to ascribe the reduced diffusion coefficients within cells to the barrier effects of the high molecular weight proteins there. Other investigators (e.g. Abetsedarskaya, et. al.¹⁰) have argued similarly.

It is interesting that diffusion is much more rapid in the muscles than in the single cells, although the solids content is nearly the same in both cases. Apparently the

⁸ J. E. Tanner, *Macromolecules* 4, 748 (1971).

⁹ B. D. Boss, E. O. Stejskal, and J. D. Ferry, *J. Phys. Chem.* 71, 1501 (1967).

¹⁰ L. A. Abetsedarskaya, F. G. Miftakhutdinova, and V. D. Fedotov, *Biophysics* 13, 750 (1968).

proteins are arranged in such a manner as not to impede diffusion within muscle cells. This is plausible considering the function of muscle cells.

The fact that the values of D_0 for the three types of single cells are nearly equal is probably fortuitous. Other single cells could probably be found which would give significantly different values.

Relaxation Measurements

A number of measurements of spin-spin (T_2) and spin-lattice (T_1) relaxation time were also performed on the samples. Some of these are presented in Figure 6. The results are all lower than the value $T_1 = T_2 = 3$ sec for pure oxygen-free water at this temperature. ($T_1 = T_2 \approx 1\frac{1}{2}$ sec for air-saturated water. However, it is probable that cell metabolism has removed most of the oxygen from within the cells.) This is an indication of restrictions to the molecular motion of the water. $T_1 \gg T_2$ is consistent with a small fraction of molecules with very restricted motion, perhaps adsorbed on various macromolecules in the cells. The values of T_1 would be much less affected than those of T_2 by such a fraction of low mobility, and it may be noted that, comparing the single cell and the muscle samples with pure water (Table 1), T_1 and D are found to decrease proportionately, indicating that for bulk water molecules the rotational motions are not slowed more than the diffusional motions by the other cell components.

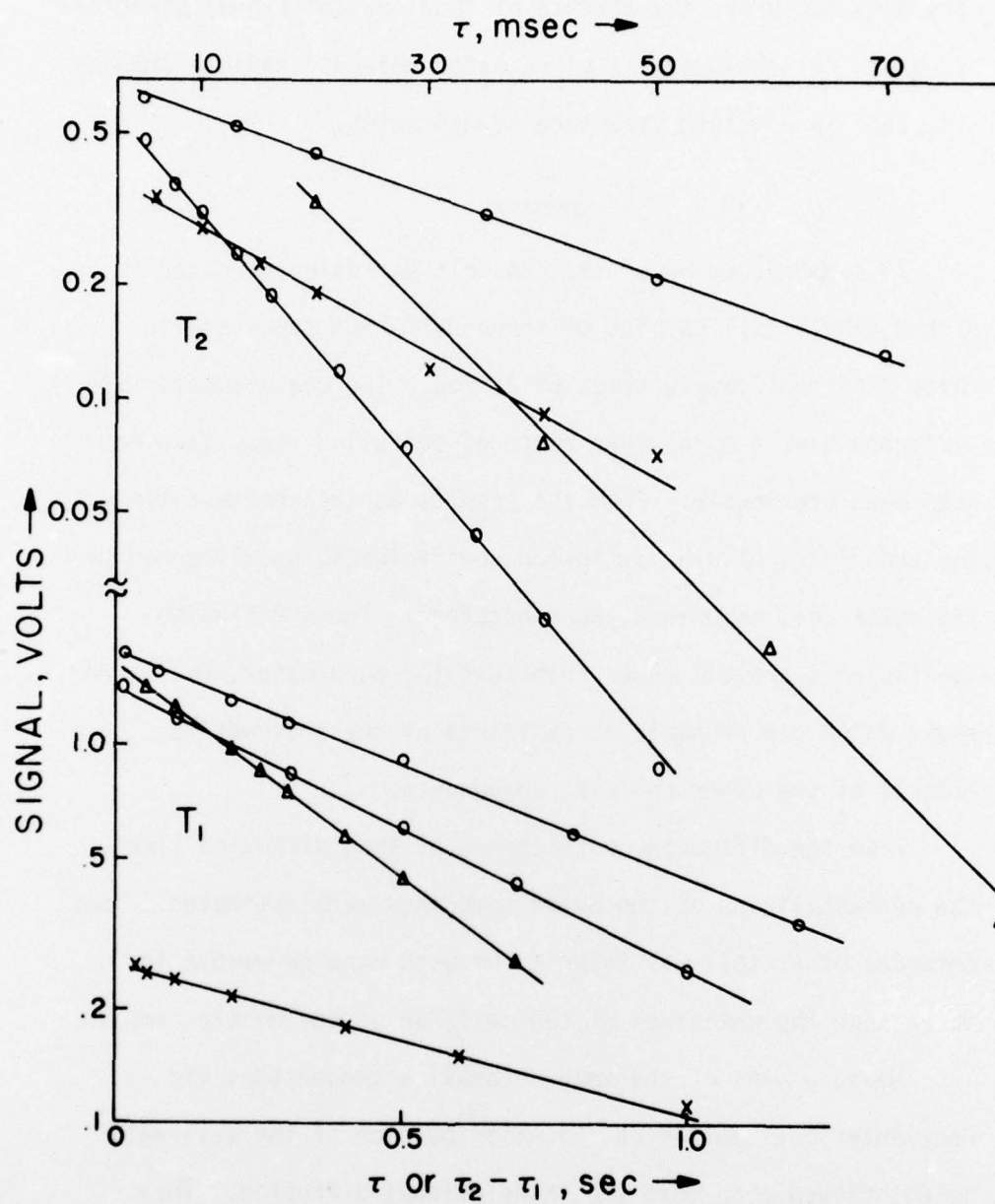


Figure 6. Representative signal decay curves due to T_1 and T_2 . The symbols are: o, red cells; O, E. coli; Δ , yeast; x, frog² muscle.

This does not prove the absence of local orientational structure of water, but shows that a given water molecule rapidly changes its place in any such structure as may exist.

SUMMARY

In summary, we have measured self diffusion of water in packed single cell samples of three different types and in three different muscle types of a frog. The measurements were performed over a much wider range of diffusion times than has been done previously. From the results at the shortest times, the true intracellular diffusion coefficients, uninfluenced by the outer cell membranes, were obtained. These diffusion coefficients are all lower than that for pure water, but by an amount which can probably be explained by the obstructive effects of the other cellular components.

From the diffusion coefficients at long diffusion times, the permeabilities of the outer membranes were estimated. The membrane of *E. coli* was found to be much more permeable to water than the membranes of red cells or of the muscle samples.

Measurements of the spin relaxation showed that the reorientational motion of the major portion of the cell water is not slowed more than the translational diffusion. They also indicate the presence of a small fraction of adsorbed water.

Work has started on deriving a rigorous expression for diffusion coefficient versus diffusion time for the case of planar barriers of arbitrary permeability.

DISTRIBUTION LIST

<u>ADDRESS</u>	<u>COPIES</u>
Administrator, Defense Documentation Center Cameron Station Alexandria, Virginia 22314	12
Director, Naval Research Laboratory Attention: Technical Information Division Code 2027 Washington, D. C. 20390	6
Director, Naval Research Laboratory Attention: Library Code 2029 (ONRL) Washington, D. C. 20390	6
Office of Naval Research Medicine and Dentistry Code 444 Arlington, Virginia 22217	3
Director, Research Division Bureau of Medicine and Surgery Department of the Navy Washington, D. C. 20390	2
Technical Reference Library Naval Medical Research Institute National Naval Medical Center Bethesda, Maryland 20014	2
Office of Naval Research Branch Office 495 Summer Street Boston, Massachusetts 02100	1
Office of Naval Research Branch Office 536 South Clark Street Chicago, Illinois 60605	1
Office of Naval Research Branch Office 1030 East Green Street Pasadena, California 91101	1
Office of Naval Research Contract Administrator for Southeastern Area 2110 G Street, N.W. Washington, D. C. 20007	1

DISTRIBUTION LIST (cont.)

<u>ADDRESS</u>	<u>COPIES</u>
Commanding Officer U.S. Naval Medical Research Unit No. 2 Box 14 APO San Francisco 96263	1
Commanding Officer U.S. Naval Medical Research Unit No. 3 FPO New York 09527	1
Officer in Charge U.S. Naval Medical Research Unit No. 4 U.S. Naval Hospital Great Lakes, Illinois 60088	1
Officer in Charge Submarine Medical Research Laboratory U.S. Naval Submarine Base, New London Groton, Connecticut 06342	1
Scientific Library U.S. Naval Medical Field Research Laboratory Camp Lejeune, North Carolina 28542	1
Scientific Library Naval Aerospace Medical Research Institute Naval Aerospace Medical Center Pensacola, Florida 32512	1
Commanding Officer U.S. Naval Air Development Center Attention: Aerospace Medical Research Department Johnsville, Warminster, Pennsylvania 18974	1
Scientific Library Naval Biomedical Research Laboratory Naval Supply Center Oakland, California 94625	1
Director, Life Sciences Division Army Research Office 3045 Columbia Pike Arlington, Virginia 22204	1
Director, Life Sciences Division Air Force Office of Scientific Research 1400 Wilson Boulevard Arlington, Virginia 22209	1

DISTRIBUTION LIST (cont.)

<u>ADDRESS</u>	<u>COPIES</u>
Commanding General U.S. Army Medical Research & Development Command Forrestal Building Washington, D. C. 20314	1
Professor H. R. Mahler Department of Chemistry Indiana University Bloomington, Indiana 47401	1
Professor Arthur Koch Department of Microbiology Indiana University Bloomington, Indiana 47401	1
Commander Naval Air System Command Department of the Navy Washington, D. C. 20361 Attention: Code AIR-954, Technical Library	2
Code AIR-310C, Dr. H. Rosenwasser	1
Commander Naval Sea Systems Command Naval Sea Systems Command Headquarters Washington, D. C. 20362 Attention: Code SEA-09G3, Technical Library	2
Code SEA-0332, Dr. A. B. Amster	1
Commander Naval Weapons Center China Lake, California 93555 Attention: Code 533, Technical Library	2
Code 60, Dr. H. W. Hunter	1
Commander Air Force Avionics Laboratory Wright-Patterson Air Force Base Ohio 45433 Attention: Code AFAL/CC	1
Commander Wright-Patterson Air Force Base Ohio 45433 Attention: Code AFWAL/DO, Technical Library	1

DISTRIBUTION LIST (cont.)

<u>ADDRESS</u>	<u>COPIES</u>
Commander Naval Surface Weapons Center White Oak Laboratory Silver Spring, Maryland 20910 Attention: Code 230, Dr. L. A. Kaplan	1
Code 250, Dr. W. McQuiston	1
Code WX-21, Technical Library	1
Commander Army Aviation Systems Command Avionics and Weaponization Division St. Louis, Missouri 63166 Attention: Code DRSAB-EVW	1
Commanding General U.S. Army Tank Automotive Command Warren, Michigan 48090 Attention: Code DRSTA-RHFL	1
Commander Naval Surface Weapons Center Dahlgren Laboratory Dahlgren, Virginia 22448 Attention: Code DG-30, Mr. R. Morrisette	1
Commanding Officer Frankford Arsenal Philadelphia, Pennsylvania 19173 Attention: Code SARFA-MDP-Y, Mr. W. Puchalski	1
Commanding Officer Edgewood Arsenal Aberdeen Proving Ground, Maryland 21010 Attention: Code SAREA-DE-MMP, Mr. M. Penn	1
Commander Ballistic Research Laboratories Interior Ballistics Laboratory Aberdeen Proving Ground, Maryland 21005 Attention: Code AMXBR-IB, Mr. J. R. Ward	1
Commander Aeronautical Systems Division (AFSC) Wright-Patterson Air Force Base Ohio 45433 Attention: Code ASD/ENAMC, Mr. M. Edelman	1

DISTRIBUTION LIST (cont.)

<u>ADDRESS</u>	<u>COPIES</u>
Commanding Officer Picatinny Arsenal Dover, New Jersey 07801 Attention: Code SARPA-FR-E-L, Mr. T. Boxer	1
Code SARPA-FR-E-L-C, Dr. F. Taylor	1
Code SARPA-TS-S, Technical Library	1
Commander Armament Development and Test Center Eglin Air Force Base Florida 32542 Attention: Code ADTC/SD3E	1
Commander Air Force Armament Laboratory Eglin Air Force Base Florida 32542 Attention: Code AFATL/DLJW, Mr. A. Beach	1
Commander Naval Ordnance Station Indian Head, Maryland 20640	1
Commander Rome Air Development Center Griffiss Air Force Base New York 13441	1
The Johns Hopkins University Applied Physics Laboratory 3621 Georgia Avenue Silver Spring, Maryland 20910 Attention: Library Acquisitions: Bldg. 5, Rm 26	1
Environmental Research Institute of Michigan P.O. Box 618 Ann Arbor, Michigan 48107 Attention: IRIA Library	1
Battelle Memorial Institute TACTEC Columbus, Ohio 43201 Attention: Ms. Nancy Hall	1
National Aeronautics and Space Administration Langley Research Center Hampton, Virginia 23665	

DISTRIBUTION LIST (cont.)

<u>ADDRESS</u>	<u>COPIES</u>
National Aeronautics and Space Administration Lewis Research Center 21000 Brookpark Road Cleveland, Ohio 44135	1
Denver Research Institute Laboratories for Applied Mechanics University of Denver Denver, Colorado 80210 Attention: Mr. Robert M. Blunt	1
University of Denver Chemistry Department Denver, Colorado 80210 Attention: Dr. John R. Riter	1
IIT Research Institute 10 W. 35th Street Chicago, Illinois 60616 Attention: Dr. Elliott Raisen	1
The Franklin Institute Research Laboratories Philadelphia, Pennsylvania 19103 Attention: Mr. Gunther Cohn	1
Professor A. Strickholm Department of Physiology Indiana University Bloomington, Indiana 47401	1